SLAC-PUB-11508

July/August 2005

Ultrafast X-ray Science at the Sub-Picosecond Pulse Source

Kelly J. Gaffney, for the SPPS collaboration

Stanford Synchrotron Radiation Laboratory, SLAC, Stanford University, Stanford, CA,

USA

Published in Synchrotron Radiation News

The SPPS has been the product of an international collaboration supported by the SLAC/SSRL, ANL/APS, BNL/NSLS, LLNL, HASYLAB/ DESY, and ESRF laboratories and synchrotron facilities and the University of Chicago/BIOCARS, the University of California at Berkeley, the University of Michigan, Copenhagen University, Uppsala University, Chalmers University, and Lund University. The SPPS collaboration in total has relied on the contributions of more than 50 scientists. Portions of this research were supported by the U.S. Department of Energy, Office of Basic Energy Science through direct support for the SPPS, as well as individual investigators and SSRL, a national user facility operated by Stanford University. Additional support for the construction of SPPS was provided in part by Uppsala University and the Swedish Research Council. Scientists within the collaboration have relied on financial support by the Deutsche Forschungsgemeinschaft, the European Commission through the FEMTO, X-RAY FEL PUMP-PROBE and XPOSE projects, the Wallenberg Research Link, and The Swedish Foundation for Strategic Research.

Work supported by Department of Energy contract DE-AC02-76SF00515

The ultrafast, high brightness x-ray free electron laser (XFEL) sources of the future have the potential to revolutionize the study of time dependent phenomena in the natural sciences. These linear accelerator (linac) sources will generate femtosecond (fs) x-ray pulses with peak flux comparable to conventional lasers, and far exceeding all other x-ray sources. The Stanford Linear Accelerator Center (SLAC) has pioneered the development of linac science and technology for decades, and since 2000 SLAC and the Stanford Synchrotron Radiation Laboratory (SSRL) have focused on the development of linac based ultrafast electron and x-ray sources. This development effort has led to the creation of a new x-ray source, called the Sub-Picosecond Pulse Source (SPPS), which became operational in 2003 [1]. The SPPS represents the first step toward the world's first hard x-ray free electron laser (XFEL), the Linac Coherent Light Source (LCLS), due to begin operation at SLAC in 2009.

The SPPS relies on the same linac-based acceleration and electron bunch compression schemes that will be used at the LCLS to generate ultrashort, ultrahigh peak brightness electron bunches [2]. This involves creating an energy chirp on the electron bunch during acceleration and subsequent compression of the bunch in a series of energy-dispersive magnetic chicanes to create 80 fs electron pulses. The SPPS has provided an excellent opportunity to demonstrate the viability of these electron bunch compression schemes and to pursue goals relevant to the utilization and validation of XFEL light sources.

Attaining time synchronization between an external laser and linac generated x-rays will be critical for the full utilization of the LCLS and other accelerator based

ultrafast x-ray sources. Studying dynamics in the time domain requires the prompt excitation and subsequent monitoring of the sample response to excitation. For structural dynamics, the fs to ps time scales of vibration, rotation, and short range translation set the required experimental resolution and necessitate stroboscopic techniques that use pulses to excite and monitor the sample. To resolve a given motion, the pulse durations must be shorter than the time scale of the motion and the pulse synchronization must be stable to better than the time scale of the motion.

Pump-probe techniques provide the dominant approach to studying ultrafast phenomena. These techniques involve excitation of a sample with an ultrafast laser pump pulse and subsequent monitoring of the sample's response with a probe pulse. When the pump and probe originate from the same source they are intrinsically time synchronous and accurate sub-fs time delays can be achieved by varying the relative path lengths of the pump and probe to the sample. For many experiments at XFEL light sources, the pump and probe will not be intrinsically synchronous. The tremendous capacity of an optical laser pump to generate a versatile range of transient states of matter and the detailed atomic and electronic structural information that can be accessed with an x-ray probe makes the merger of these two experimental capacities an important objective for the SPPS and future XFEL sources. Without inherent time synchronization, laser pump x-ray probe experiments require the relative time delay to be measured for each pump-probe pulse pair. At the SPPS, we have developed and demonstrated an electro-optic sampling technique capable of determining the relative arrival time of the laser and x-ray pulses with an accuracy better than100 fs [3].

We have also conducted experiments at the SPPS that highlight the power of ultrafast x-ray sources for studying structural dynamics with atomic detail and help validate the coming investment in XFEL facilities. This has been achieved by studying the dynamics of electronically driven melting in a semiconducting InSb crystal [4]. In these experiments, we have used ultrafast x-ray diffraction to clarify the dynamical pathway for non-thermal melting with unprecedented detail.

I. Time Synchronization with Electro-Optic Sampling

Experiments that wish to utilize the tremendous flexibility and precision of laser excitation with the atomic structural detail of x-ray science will require the accurate time synchronization of these two independent light sources. Active stabilization of the laser repetition rate to a harmonic of the radio frequency (RF) used to accelerate electrons in the SLAC linac synchronizes the sources, but noise in the RF and jitter between the RF, electron bunches, and laser pulses will result in an imperfect synchronization that degrades the temporal resolution. Given the sub-100 fs durations of the x-ray and laser pulses at the SPPS, this jitter in the synchronization becomes the resolution limit for any experiment that requires the averaging of more than one pump-probe pulse pair. The full utilization of XFEL radiation requires the development of techniques that can monitor the pulse to pulse fluctuations in laser-XFEL synchronization to an accuracy comparable to the pulse durations used in the experiments.

The SPPS collaboration has developed a non-invasive technique based on electro-optic sampling (EOS) to cross correlate the laser and electron bunch arrival times in an electro-optic (EO) ZnTe crystal [3, 5-9]. In EOS the electromagnetic fields associated

with the electron bunch anisotropically distort the index of refraction in the electro-optic crystal that sits in close proximity to the electron beam. These fields generate a transient birefringence in the crystal that tracks the temporal profile of the bunch charge. This transient birefringence in the crystal will imprint the arrival time of an electron bunch on the laser polarization if the laser pulse and electric field have a time coincident arrival at the crystal. A polarizer then separates the rotated light from the unaffected light. By nulling the laser intensity along one polarization direction in the absence of any transient birefringence, the appearance of laser intensity along this polarization direction signals the time coincident arrival of the laser and electron pulses.

EOS measures the relative arrival time for each pair of pulses by using a crossed beam geometry, as shown in Figure 1. This causes the laser arrival time to vary across the EO crystal relative to the electron bunch electric field, mapping temporal delay into a spatial coordinate which can be imaged onto a CCD array detector [6]. The spatial position of the EOS signal indicates the time at which the peak of the laser intensity matches the peak in the electronic field strength.

The shot-to-shot fluctuations in relative timing measured with EOS appear in Figure 2(A). The centroid of each EO image can be determined with 30 fs accuracy. Figure 2(B) shows a histogram of arrival times measured in a one hundred second time period. The Gaussian fit has a standard deviation of 200 fs. These measurements demonstrate the power of EOS as an electron beam diagnostic. To determine the value of the technique for determining the relative arrival time of an amplified laser pulse and an x-ray pulse in the x-ray experimental station we compared the jitter in the arrival time

measured with EOS to that measured with a laser-pump-x-ray probe study of ultrafast non-thermal melting.

Intense excitation of semiconducting crystals with a fs laser pulse will disorder and melt the crystal, significantly reducing the diffracted x-ray intensity in a few hundred fs [4, 10-13]. These melting studies also used a crossed beam geometry, like that shown in Figure 1. The x-ray and laser pulses approach the InSb surface with different angles of incidence, causing them to sweep across the surface of the crystal with different rates. This imprints a range of pump-probe delays on the surface of the crystal, creating a spatial axis that doubles as a temporal axis. Imaging the spatial profile of the diffracted x-ray intensity with a CCD array provides the time history around t=0 in a single shot. As the time of arrival fluctuates from shot-to-shot, the spatial location of the decay in diffracted intensity will shift, providing a direct monitor of the arrival time with an accuracy of 50 fs and a means of testing the correlation between the jitter measured with EOS and the jitter between the laser and x-ray pulses measured in the x-ray hutch. The comparison of data collected over a 30 second period appears in Figure 3. While each technique yields a jitter with a standard deviation of approximately 200 fs, the correlation of the two measurements has a standard deviation of only 60 fs. This demonstrates the viability of using the EOS time of arrival to bin a pump-probe signal and collect time averaged data with a time resolution better than the timing jitter.

II. Atomic Scale Visualization of a Laser Driven Phase Transition

The past twenty years have seen our understanding of structural dynamics increase significantly because of the advent of laser spectroscopy with fs time resolution.

For a limited number of simple physical and chemical transformations, such as uni-molecular, diatomic reactions in the gas phase [14], ultrafast studies of electronic transitions provide a detailed picture of nuclear dynamics during chemical reaction. For more complex materials and phenomena, ultrafast spectroscopy continues to be a useful tool for studying structural dynamics, but it no longer provides an unambiguous picture of the structural evolution.

This is a direct consequence of the daunting number of degrees of freedom in the vast majority of condensed phase transformations. Ultrafast studies of laser excited crystalline semiconductors provide an extensively studied example of the limitations of ultrafast spectroscopy [13, 15-17]. While intense optical excitation generates metal-like reflectivities consistent with the metallic liquid phase, transient reflectivities provide an indirect and inconclusive probe of atomic structure that cannot definitively signal the onset of liquid formation nor the structural pathway followed during the phase transformation.

The interesting range of structural phenomena inferred from these optical measurements [13, 15-17] has lead to a series of ultrafast x-ray diffraction experiments that have used an ultrafast laser to generate a plasma and produce x-ray pulses for probing structural dynamics in optical laser excited crystals [10-12]. These pioneering experiments have shown crystal disordering to occur on the ultrafast time scale, including disordering faster than the time scale for energy transfer from the excited carriers to the lattice, but they have neither identified the atomic motions that lead to disordering nor determined the time needed to generate liquid-like structure and dynamics.

Ultrafast x-ray diffraction studies at the SPPS of laser driven melting in an InSb semiconducting crystal have moved beyond the validation of the proposed electronically driven phase transition to experimentally characterizing the atomic motions that lead to crystal disordering [4]. In order to overcome fluctuations in the arrival times of the x-ray and laser pulses, we measured the relevant time evolution with a crossed beam geometry discussed in Section I and analogous to that shown in Figure 1 for electro-optic sampling.

Using an asymmetrically cut crystal allows for an x-ray incidence angle of 0.4^{o} with respect to the crystal surface. The grazing incidence angle matches the x-ray and laser penetration depths and greatly reduces the contribution of unexcited sample to the diffraction signal. Figure 4(A) shows the time dependent x-ray diffraction intensity from a laser excited crystal for both the (111) and (220) reflections. The diffracted intensity decays non-exponentially and can be well fit to a Gaussian, $I(Q,t) = \exp\left(-\frac{t^2}{\tau^2}\right)$ for $0 < t < 500$ fs. As shown in Figure 4(A), the (220) Bragg peak decays faster than the (111). The fit gives time constants, , of 280 and 430 fs for the (220) and (111) reflections. The ratio of these time constants, $_{111}/\ _{220} = 1.5 \pm 0.2$, equals the ratio of the magnitude of the reciprocal lattice vectors for the two reflections ($\sqrt{8/3}$).

This inverse-*Q*-dependent scaling and Gaussian time dependence strongly implies statistical, atomic motion that can be described using a time-dependent Debye-Waller-like model that relates the time dependent decrease in diffracted intensity to a time-dependent root mean square (rms) displacement, $I(Q,t) = \exp\left(-Q^2 \left\langle u^2(t) \right\rangle / 3\right)$, where Q is the reciprocal lattice vector and $\left\langle u^2(t) \right\rangle$ is the time-dependent mean-square displacement of the photo-excited atoms, averaged spatially over the sample. The time

dependent root mean square (rms) displacement appears in Figure 4(B) for the (111) and the (220) reflections. For the first few hundred fs, the rms displacement in these two directions have identical time dependence and increase linearly with time. This linear time dependence demonstrates that the initial disordering results from inertial atomic motion on the laser modified potential. The momentum of the ions does not change upon laser excitation, in accordance with the Franck-Condon principle. Thus the atoms will initially sample the new potential energy surface with a velocity distribution dictated by the lattice temperature prior to laser excitation. This predicts the rms displacement should increase linearly with time, with an average velocity determined by the average atomic mass and the temperature. For InSb at room temperature, the predicted slope of $\left(\frac{3k_BT}{M}\right)^{1/2} = 2.5$ Å/ps agrees reasonably well with the experimental value of 2.3±0.2 Å/ps.

The amplitude of the inertial response indicates the magnitude of the lattice softening, since the lattice temperature remains constant during inertial motion and the rms displacement is inversely proportional to the average frequency of the thermally excited phonons. The inertially accessible rms displacement exceeds the ground state rms displacement of 0.16 Å by nearly an order of magnitude, as shown in Figure 4(B). Interestingly, these large displacements that occur during the first few hundred fs result in an increased disorder, but not a transition to a liquid like structure because these inertial motions preserve the atomic memory of the initial lattice configuration. Only after velocity randomizing collisions can the structure begin to lose translational symmetry.

III. Summation

X-ray free electron lasers possess the capacity to transform the study of dynamic phenomena in biology, chemistry, and physics. The Sub-Picosecond Pulse Source has provided an opportunity to develop and demonstrate an electro-optic sampling method capable of determining the relative arrival times of an ultrafast laser and x-ray pulse to roughly a 60 fs accuracy [3], a capability that will be essential to many proposed experiments at XFEL light sources. The SPPS has also provided an opportunity to demonstrate how an ultrafast hard x-ray source with high peak brightness can clarify the evolution of atomic structure during a physical or chemical transformation with unprecedented detail [4].

The SPPS has been the product of an international collaboration supported by the SLAC/SSRL, ANL/APS, BNL/NSLS, LLNL, HASYLAB/ DESY, and ESRF laboratories and synchrotron facilities and the University of Chicago/BIOCARS, the University of California at Berkeley, the University of Michigan, Copenhagen University, Uppsala University, Chalmers University, and Lund University. The SPPS collaboration in total has relied on the contributions of more than 50 scientists. Portions of this research were supported by the U.S. Department of Energy, Office of Basic Energy Science through direct support for the SPPS, as well as individual investigators and SSRL, a national user facility operated by Stanford University. Additional support for the construction of SPPS was provided in part by Uppsala University and the Swedish Research Council. Scientists within the collaboration have relied on financial support by the Deutsche Forschungsgemeinschaft, the European Commission through the FEMTO, X-RAY FEL PUMP-PROBE and XPOSE projects, the Wallenberg Research Link, and The Swedish Foundation for Strategic Research.

References:

1. M. Cornacchia, et al., *A Sub-Picosecond Photon Pulse Facility for SLAC* (SLAC-PUB-9850, 2001)
2. P. Krejcik, et al., in *Proceeding of the 2003 Particle Accelerator Conference*, edited by J. Chew, S. Lucas and S. Webber (IEEE, Piscataway, NJ, IEEE, Portland, OR, 2003), p. 423.
3. A. L. Cavalieri, et al. Clocking femtosecond x rays. *Phys. Rev. Lett.* **94,**(2005).
4. A. M. Lindenberg, et al. Atomic-Scale Visualization of Inertial Dynamics. *Science* **308,**392-395 (2005).
5. J. A. Valdmanis and G. Mourou Subpicosecond Electrooptic Sampling - Principles and Applications. *IEEE J. Quantum Electron.* **22,**69-78 (1986).
6. J. Shan, et al. Single-shot measurement of terahertz electromagnetic pulses by use of electro-optic sampling. *Optics Letters* **25,**426-428 (2000).
7. M. J. Fitch, et al. EIectro-optic measurement of the wake fields of a relativistic electron beam. *Phys. Rev. Lett.* **8703,**(2001).
8. I. Wilke, et al. Single-shot electron-beam bunch length measurements. *Phys. Rev. Lett.* **88,**(2002).
9. G. Berden, et al. Electro-optic technique with improved time resolution for real-time, nondestructive, single-shot measurements of femtosecond electron bunch profiles. *Phys. Rev. Lett.* **93,**(2004).
10. C. W. Siders, et al. Detection of nonthermal melting by ultrafast X-ray diffraction. *Science* **286,**1340-1342 (1999).
11. A. Rousse, et al. Non-thermal melting in semiconductors measured at femtosecond resolution. *Nature* **410,**65-68 (2001).
12. K. Sokolowski-Tinten, et al. Femtosecond x-ray measurement of ultrafast melting and large acoustic transients. *Phys. Rev. Lett.* **87,**225701 (2001).
13. S. K. Sundaram and E. Mazur Inducing and probing non-thermal transitions in semiconductors using femtosecond laser pulses. *Nature Mater.* **1,**217-224 (2002).
14. A. H. Zewail Laser Femtochemistry. *Science* **242,**1645-1653 (1988).
15. P. Saeta, et al. Ultrafast electronic disordering during femtosecond laser melting of GaAs. *Phys. Rev. Lett.* **67,**1023-1026 (1991).
16. K. Sokolowski-Tinten, J. Bialkowski and D. von der Linde Ultrafast laser-induced order-disorder transitions in semiconductors. *Phys. Rev. B* **51,**14186-14198 (1995).
17. A. M. T. Kim, J. P. Callan, C. A. D. Roeser and E. Mazur Ultrafast dynamics and phase changes in crystalline and amorphous GaAs. *Phys. Rev. B* **66,**(2002).

Figure Captions:

Figure 1: Crossed beam geometry used in spatially resolved electro-optic sampling. The blue, red, and black objects represent the EO crystal, the ultrafast laser pulse, and the ultra-relativistic electron bunch (with electric field lines indicated), respectively. The purple laser light represents the laser light influenced by the electron bunch electric field. (A) The laser arrives late with respect to the electron bunch arrival, generating an electro-optic signal at the top of the laser pulse. (B) The laser arrives earlier with respect to the electron bunch arrival, generating an electro-optic signal towards the bottom of the laser pulse. (C) The spatial variation of the laser polarization reflects the temporal profile of the electron bunch. Also plotted is the spatial variation of the intensity of two orthogonal laser polarizations. The motion of the centroid of the signal from shot-to-shot provides a measure of the jitter in the laser pulse electron bunch arrival times.

Figure 2: (A) Twenty consecutive single shot measurements of the relative time of arrival for the laser-electron bunch pair. The red band in each column gives the peak of the electro-optic signal with its location indicating the time of arrival of the electron bunch with respect to the laser probe pulse. (B) The inset shows a histogram of the relative arrival times for 1000 consecutive electron bunches.

Figure 3: (A) Shot-to-shot comparison of the relative time of arrival for the laser-electron bunch pair measured with EOS in green, and the x-ray-laser pulse pair measured with laser driven melting in red. Both measurement techniques show an arrival time jitter with a ~200 fs standard deviation. (B) Correlation plot of the data shown in (A), where perfect

correlation would generate a straight line with a slope of one, as shown by the black line. The variation between the jitter measured by the two techniques has a standard deviation of 60 fs.

Figure 4: (A) Time dependent diffraction intensity for the (111) (Δ) and the (220) (○) reflections. (B) Time dependent root-mean square displacement for the (111) (Δ) and the (220) (○) reflections. A black line with a slope of 2.3 Å/ps has been plotted on the graph. Data collected with laser fluence of 130 $mJcm^{-2}$.

K.J. Gaffney Figure 1

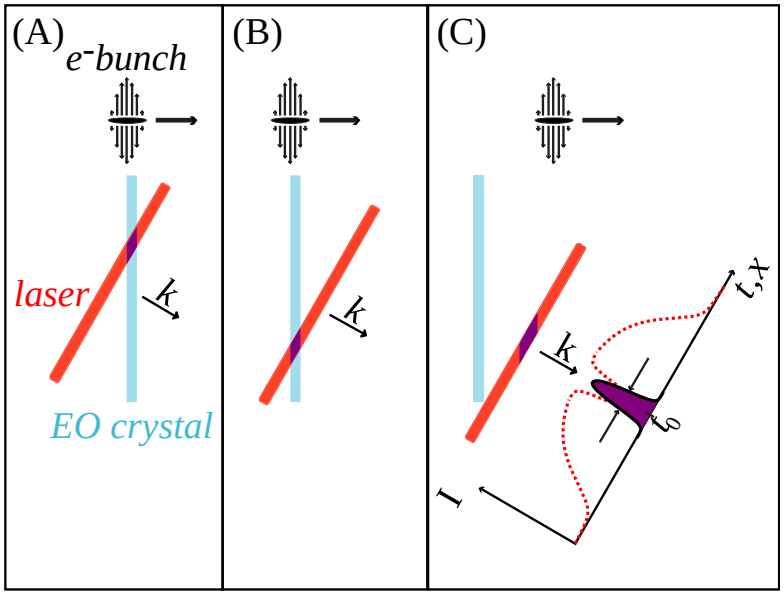

K.J. Gaffney Figure 2

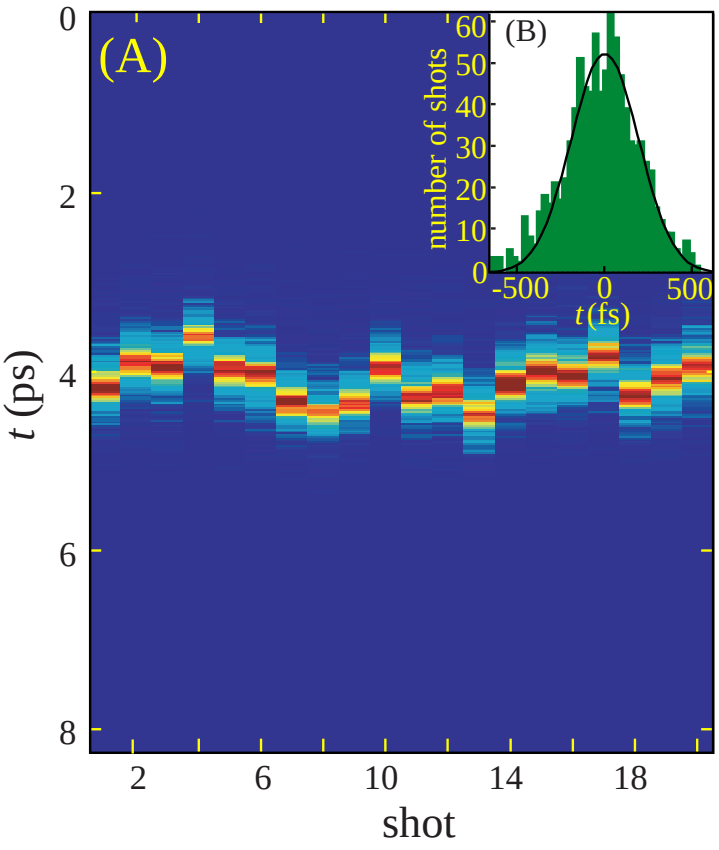

K.J. Gaffney Figure 3

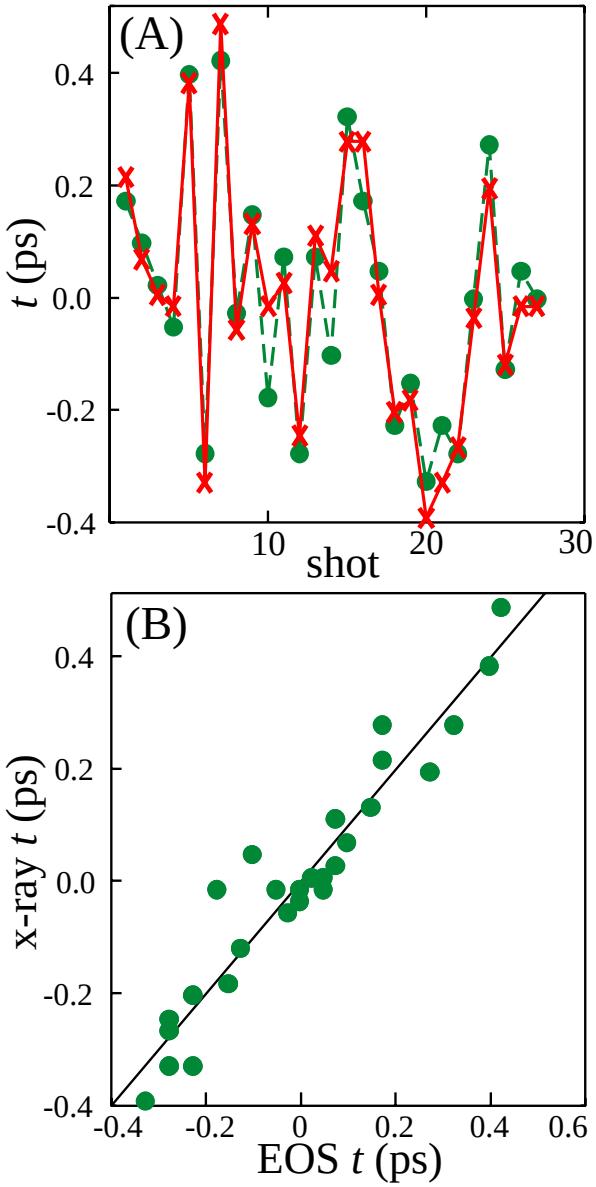

K.J. Gaffney Figure 4